

# THE REMOVAL OF ONE-COMPONENT BUBBLES FROM GLASS MELTS IN A ROTATING CYLINDER

LUBOMÍR NĚMEC, VLADISLAVA TONAROVÁ

Laboratory of Inorganic Materials, Joint Workplace of the Institute of Chemical Technology Prague and the Institute of Inorganic Chemistry AS CR Technická 5, 166 28 Prague, Czech Republic

E-mail: Lubomir.Nemec@vscht.cz

Submitted May, 4; accepted July 15, 2006

**Keywords:** Glass melt, Bubble, removal, Centrifugal force

*The bubbles containing pure oxygen or carbon dioxide were investigated in a rotating cylinder containing glass melt. The equation of one component bubble with steady concentration gradient of gas on the bubble surface was applied, taking into account the effect of centrifugal force. The impact of the cylinder rotation velocity, the degree of its filling by the melt, cylinder radius, temperature, bubble size and bubble initial position in the cylinder on the bubble removal time from the melt was calculated with the aim to find theoretical advantageous conditions of the bubble removal process. Both mechanism of bubble removal, namely bubble dissolution and bubble separation to the cylinder centre, were found and evaluated. The mechanism preference depended primarily on the bubble initial composition. The dissolution mechanism was crucial for in glass well soluble gas as is oxygen whereas less soluble carbon dioxide exhibited only the mechanism of bubble separation. Both mechanisms were particularly accelerated by increasing the cylinder rotation velocity. The application of centrifugal fining needs the investigation of multicomponent bubbles with composition corresponding to bubbles under real melting conditions.*

## INTRODUCTION

In the last work, the equations describing the behavior of small bubbles in a glass melt under effect of both gravitational and centrifugal forces were derived [1]. The increasing effort of glass technologists to accelerate and economize the industrial glass melting process, as well as the ingoing production of high quality glasses, evoke an address to non traditional ways of glass fining. The novel concepts frequently aim at avoiding the refining agents owing to their contamination effect in both glass and environment. The replacement of the classical refining agent by an inert rapidly diffusing gas [2] or the application of reduced pressure [3-5] are means how to ensure bubble growth and their accelerated removal from glass by rising. The application of an additional force field influencing bubble behavior, such as supersonic energy [6] or centrifugal force, is a further way leading to the physical acceleration of the fining process. The application of rotating spaces containing glass melt is a promising concept, particularly for special glasses produced in a low or medium scale and preferably without a continual production. This work deals with bubble removal from a model rotating cylinder partially filled with the glass for the production of television bulbs as a model glass melt. Two representative gases were chosen as a content of one-component bubbles in the glass melt: oxygen representing a well soluble gas in the melt owing to its chem-

ical reaction with oxidation-reduction components of glass, and carbon dioxide, the most usual gas in glass melting, mostly physically soluble in glass melts. The influence of different process parameters on the bubble removal process was calculated by using appropriate bubble equations. The examined parameters were the cylinder rotation velocity, the cylinder radius, the degree of cylinder filling by the melt, temperature, bubble size and bubble initial position in the cylinder. The bubble removal time from the melt by any removal mechanism was calculated to reveal parameter significance and process feasibility.

## THEORETICAL

### The single one-component bubble behavior

A bubble containing pure gas is considered located in a rotating vertical cylinder with glass melt. The glass in the cylinder is quiescent (discontinual process). The positive directions of movement are towards the cylinder bottom and to its periphery as it is apparent from figure 1a. The shapes of melt level at higher angle velocities are presented in figure 1b. Under the effect of the gravitational field only, the bubble will move upwards. The bubble movement in the simultaneous centrifugal field adds a radial component of bubble in direction of the cylinder centre. For a single bubble con-

taining only one gas, the equation providing the rate of bubble dissolution or growth rate is given by the derivative of the Gay Lussac's equation for the bubble volume [1]:

$$\frac{da}{d\tau} = \frac{RT}{4\pi M_i p_i a^2} \frac{dm}{d\tau} + \frac{2\omega^4 r^2 \rho^2 a^3}{27\eta p_i} + \frac{2g^2 \rho^2 a^3}{27\eta p_i} + \frac{a}{3T} \frac{dT}{d\tau} \quad (1)$$

where  $a$  is the bubble radius,  $\tau$  is time,  $R$  is the universal gas constant,  $T$  is temperature in K,  $M_i$  is the molecular mass of the  $i$ -th gas,  $p_i$  is the total pressure inside the bubble,  $m$  is the mass of gas in the bubble,  $\omega$  is the cylinder angle velocity,  $r$  is the radial distance,  $\rho$  and  $\eta$  are glass density and dynamic viscosity.

The total pressure inside the cylinder is [1]:

$$p_i = p_{ex} + \rho gh + \frac{\rho \omega^2 r^2}{2} + \frac{2\sigma}{a} \quad (2)$$

where  $p_{ex}$  is the external pressure,  $h$  is the bubble depth under glass level and  $\sigma$  is the surface tension of the melt.

The bubble moving velocity involving buoyancy and the centrifugal component is given by:

$$v_{bub} = \frac{2\rho a^2}{9\eta} (g^2 + \omega^4 r^2)^{1/2} \quad (3)$$

The mass transfer term in equation (1) is generally given by:

$$\frac{dm}{d\tau} = 4\pi a^2 k_i (m_{ib} - m_{ia}) \quad (4)$$

where  $m_{ib}$  is the bulk concentration of gas in the melt,  $m_{ia}$  is its concentration on the bubble boundary and  $k_i$  is the mass transfer coefficient of gas. The value of  $m_{ia}$  according to Henry's law is given by:

$$m_{ia} = L p_i \quad (5)$$

where  $L_i$  is the gas physical solubility in the melt and  $p_i$  is its partial pressure inside bubble (for one-component bubble,  $p_i = p$ ).

According to [7], the mass transfer coefficient between moving bubble interacting with the liquid is given by:

$$k_i = \frac{Sh_i D_i}{(2a)} \quad \text{where } Sh_i = 1 + (1 + Pe_i)^{1/3} \quad (6)$$

and  $Sh_i$  and  $Pe_i$  are the Sherwood and Peclet dimensionless criteria and  $D_i$  is the diffusion coefficient of gas.

The  $Sh_i$  expresses the mass transfer between a moving bubble and the melt, whereas  $Pe_i$  demonstrates the ratio between the inertial and the diffusion forces on the bubble surface. The Peclet number of a bubble in the quiescent melt under the influence of the gravitational and centrifugal force is then given by:

$$Pe_i = \frac{2av_{bub}}{D_i} = \frac{4\rho a^3}{9\eta D_i} (g^2 + \omega^4 r^2)^{1/2} \quad (7)$$

If  $Pe_i$ , as well as  $Pe_i^{1/3} \gg 1$ , i.e. the bubble moves sufficiently fast (the case of moving in the centrifugal field), the bubble is not too small or mass transfer is slow, the mass transfer coefficient has a form:

$$k_i = \frac{0.382 D_i^{2/3} \rho^{1/3}}{\eta^{1/3}} (g^2 + \omega^4 r^2)^{1/6} \quad (8)$$

and the resulting equation is obtained after the substitution of equations (4, 5) and (8) into (1):

$$\frac{da}{d\tau} = \frac{0.382 R T D_i^{2/3} \rho^{1/3}}{M_i \eta^{1/3} p_i} (g^2 + \omega^4 r^2)^{1/6} (m_{ib} - m_{ia}) + \frac{2\omega^4 r^2 \rho^2 a^3}{27\eta p_i} + \frac{2g^2 \rho^2 a^3}{27\eta p_i} + \frac{a}{3T} \frac{dT}{d\tau} \quad (9)$$

The first, second and third term on the right side of equation (9) express the impact of mass transfer, the gravitational force and the centrifugal force, respectively, while the last term represents the influence of thermal expansion of gas.

#### The level shape in the rotating cylinder

At higher rotation velocities, the level has the shape shown in figure 1b. The values of abscissa  $h_u$ ,  $h_d$ ,  $r_u$  and  $r_d$  for this case are given by following equations [1]:

$$r_u = \left( \frac{gh_o}{\omega^2} + r_o^2 - \frac{V}{\pi h_o} \right)^{1/2} \quad (10)$$

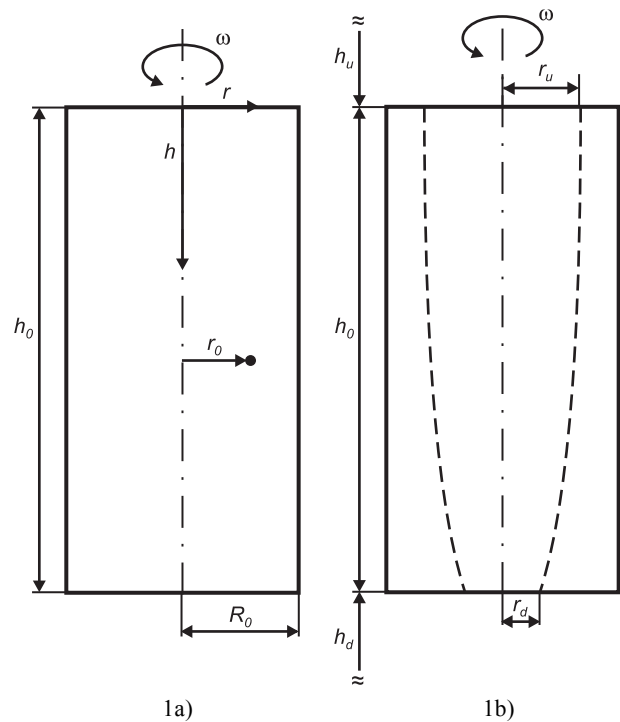


Figure 1. a) The scheme of the cylinder with positive radial and axial directions; b) The shape of glass level in the rotating cylinder at higher rotation velocities.

$$h_u = \frac{\omega^2 (r_o^2 - r_u^2)}{2g} \quad (11)$$

$$r_d = \frac{[\omega^2 r_u^2 - 2gh_o]^{1/2}}{\omega} \quad (12)$$

$$h_d = \frac{\omega^2 r_u^2}{2g} - h_o \quad (13)$$

where  $V$  is the melt volume in the cylinder.

## RESULTS OF CALCULATIONSN

### Extent of calculations and experimental data

The following calculations were realized at constant temperature, only the influence of gas diffusion and the centrifugal force on the bubble movement and growth or dissolution was considered. Consequently, the third and fourth members on the right side of equation (9) were omitted. The important factors of the bubble removal were defined and arranged into a decreasing sequence corresponding to how easily their values can be adjusted in the process:

$$\omega > V/V_o > R_o > t > c_{oi} > f(a_o), r_o(r) \quad (14)$$

where  $f(a_o)$  - the initial distribution of bubble sizes in the cylinder,  $r_o(r)$  - radial starting bubble positions,  $c_{oi}$  - the initial bubble composition,  $t$  - temperature (°C),  $R_o$  - the cylinder radius,  $V/V_o$  - filling by glass,  $\omega$  - angle velocity of the cylinder. The bubble size distribution and initial bubble positions in the melt are natural consequences of the melting process and are only hardly adjustable.

The extent of calculations involved the following quantity intervals:

$a_o$  ( $a_o \in \langle 1 \times 10^{-4}; 5 \times 10^{-4} \rangle$  m;  $a_o = 5 \times 10^{-5}$ ),  
 $r_o$  ( $r_o = 0.20; 0.225$  and  $0.25$  m),  
 $\omega$  ( $\omega = 25, 50, 100, 200$  s<sup>-1</sup>),  
 $t$  ( $t = 1300, 1400, 1500$ °C),  
 $V/V_o$  ( $V/V_o = 1; 0.75; 0.5$ ),  
 $R_o$  ( $R_o = 0.25, 0.375, 0.5$  m),  
 $h_o$  ( $h_o = 0.5$  m),  
 $c_{oi}$  ( $O_2$  as a fast diffusing and well soluble gas,  $CO_2$  as a slowly diffusing gas).

TV panel glass and both gases were characterized by the following values:

$\rho = 2790 - 0.2378T$  (kg/m<sup>3</sup>),  
 $\eta = \rho \exp[-11.501 + 6144.6/(T - 710.6)]$  (Pa.s.)  
 $D_{O_2} = \exp(-18.53 - 5755/T)$ ,  $D_{CO_2} = \exp(-14.0 - 24890/T)$   
(m<sup>2</sup>/s),  $m_{CO_2b} = 0.098$  (kg/m<sup>3</sup>),  
 $L_{O_2} = \exp(0.8372 - 5750/T)$ ,  $L_{CO_2} = \exp(-6.96 - 9100/T)$   
(kg/m<sup>3</sup> bar).

The oxygen solubility was calculated from the chemical equilibrium of oxygen with antimony ions in the melt. The following values were applied:

$t$ (°C)	1300	1400	1500
$m_{O_2b}$ (kg/m <sup>3</sup> )	0.0178	0.0902	0.1803

The time developments of the bubble radius and the bubble radial position were followed. The quantity  $\tau_{max}$  corresponding to the maximum time needed to remove a bubble either by dissolution (denoted by asterisks in pictures) or by separation to the curved glass level (denoted by circles) were used as a criterion for the fining efficiency.

### Results

In all the calculations, the time developments of the bubble radius and the bubble radial position were followed, and the resulting value of  $\tau_{max}$  was ascertained by comparison of either dissolution times or separation times of bubbles of different initial radii under given conditions. The most initial positions of bubbles in the cylinder were located on the cylinder periphery, the impact of the initial bubble radial position was examined by a series of calculations. As the standard calculation, the following conditions were chosen:  $\omega = 50$  s<sup>-1</sup>,  $V/V_o = 0.5$ ,  $R_o = r_o = 0.25$  m,  $t = 1300-1500$ °C,  $a_o \in \langle 1 \times 10^{-4} \text{ m}, 5 \times 10^{-4} \text{ m} \rangle$ . The standard gas was oxygen.

The typical courses of the bubble wandering in the form of radial distance versus time are shown in figure 2. Only bubbles of considered minimum and maximum

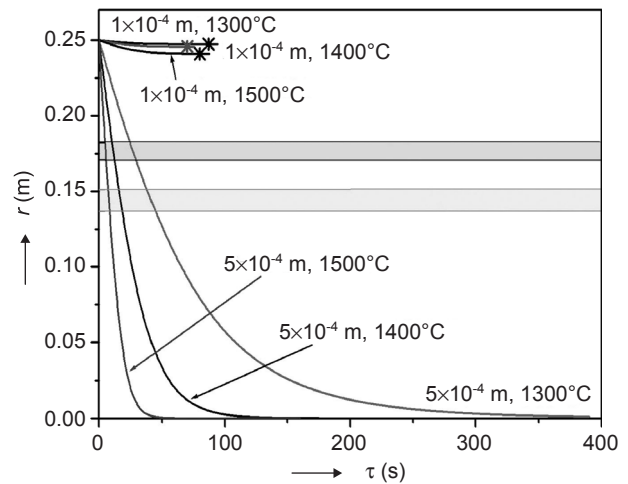


Figure 2. The typical courses of movement of oxygen bubbles from the cylinder mantel to its centre under the effect of the centrifugal force. The dependence between the bubble radial distance and time. Two grey bands correspond to the level extent for  $V/V_o = 0.5$  and  $0.75$ .  $R_o = 0.25$  m. The initial bubble radius is  $a_o = 1 \times 10^{-4}$  m;  $5 \times 10^{-4}$  m.

bubble sizes are plotted in the figure. The two grey horizontal bands in the figure correspond to the radial interval of glass levels at  $V/V_0 = 0.5$  and  $V/V_0 = 0.75$  (see figure 1b). The bubble is separated from the melt when reaching its proper position in the grey band, dependent on its initial depth under glass level. The asterisks in the figure denote the bubble dissolution. The slowing down of the bubble movement towards the cylinder centre is obvious during later stages. This is a consequence of a decreasing effect of the centrifugal force. Therefore partial filling of the cylinder by the melt appears to be only precondition for an effective bubble separation. Figure 3 provides the picture of the same case in the form of bubble radii versus time. The almost linear dissolution of small oxygen bubbles is obvious whereas bigger bub-

bles grow due to a pressure decrease inside them.  $\text{CO}_2$  bubbles exhibit a partially different behavior. The  $\text{CO}_2$  gas has only a limited solubility in the melt and the rate of its diffusion is simultaneously restricted by low values of its diffusion coefficient in the melt. That is why all bubbles, including small bubbles  $a_0 = 5 \times 10^{-5}$  m, should be separated by wandering to the glass level, nevertheless the separation of small bubbles is significantly slow as is shown in the corresponding figure 4, providing the bubble radial distance as a function of time. The very slow increase of radii of small bubbles  $a_0 = 5 \times 10^{-5}$  m is presented in figure 5.

The initial radial position of the bubble in the cylinder plays a role in the bubble removal as both pressure inside a bubble and the gas concentration gradient on its

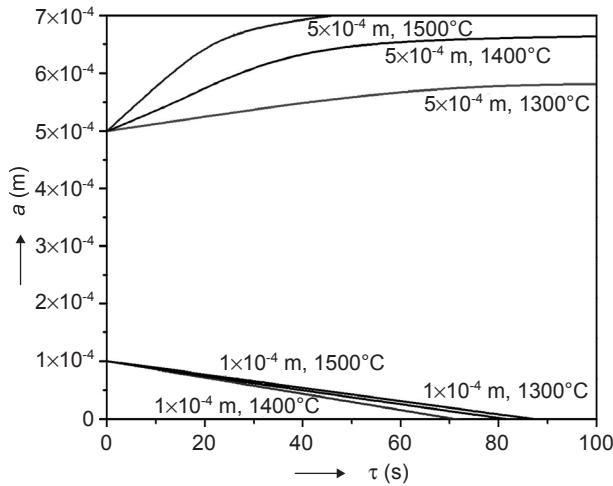


Figure 3. The typical dependences between the bubble radius and the time for bubbles wandering according to the figure 2. The initial bubble radius is  $a_0 = 1 \times 10^{-4}$  m;  $5 \times 10^{-4}$  m.

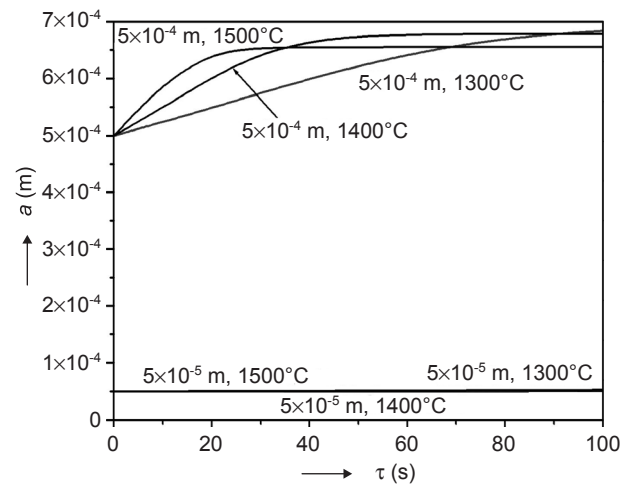


Figure 5. The typical dependences between radii of  $\text{CO}_2$  bubbles and the time corresponding to bubbles in figure 4.

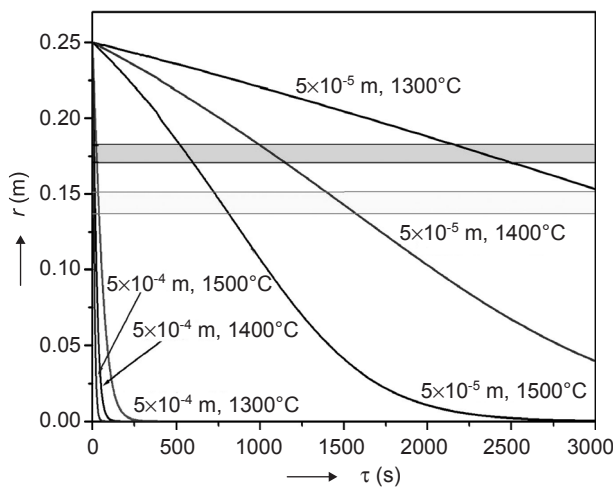


Figure 4. The courses of the separation of  $\text{CO}_2$  bubbles in the rotating cylinder. The dependence between the bubble radial distance and time.  $V/V_0 = 0.5$ ,  $R_0 = 0.25$  m.

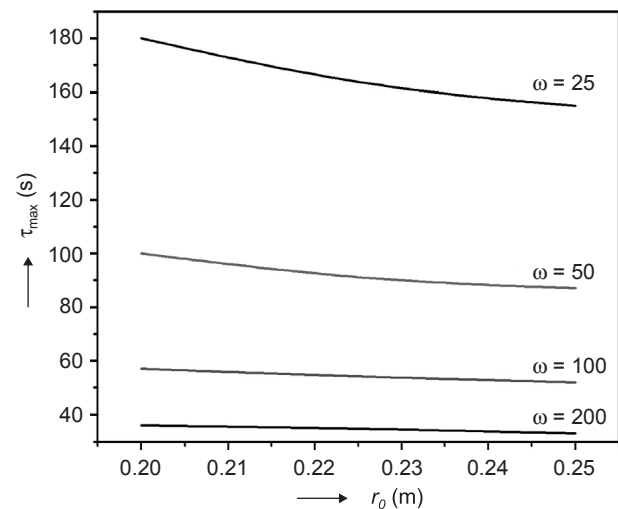


Figure 6. The dependence between the dissolution times of small oxygen bubbles and their initial radial positions in the rotating glass layer. Oxygen bubbles at  $1300^\circ\text{C}$ ,  $R_0 = 0.25$  m,  $V/V_0 = 0.5$ .

surface are affected. Figures 6 and 7 show, that the effect of the initial bubble position is dependent on the mechanism of bubble removal. The small dissolving bubbles need high internal pressure. Consequently, bubbles close to the cylinder periphery dissolve slightly faster than others in the cylinder with  $R_0 = 0.25$  m (the typical case is shown in figure 6). On the contrary, the bigger bubbles removed by the separation mechanism are separated faster if their initial distance from the cylinder centre is small. This is obvious from the figure 7. Only the mechanism of bubble separation is relevant for bubbles containing  $\text{CO}_2$ ; the character of the dependence between the bubble separation time and its initial radial distance is depicted in figure 7.

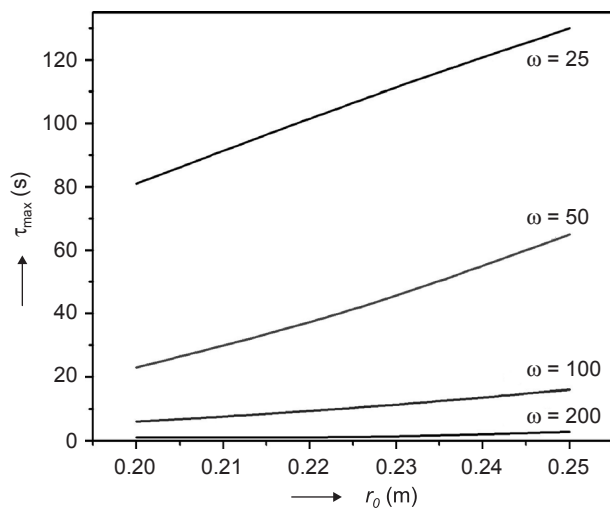


Figure 7. The dependence between the bubble separation time (regardless of the initial bubble size) to the glass level and its initial radial position in the rotating cylinder. Oxygen bubbles at  $1500^\circ\text{C}$ ,  $V/V_0 = 0.5$ ,  $R_0 = 0.25$  m.

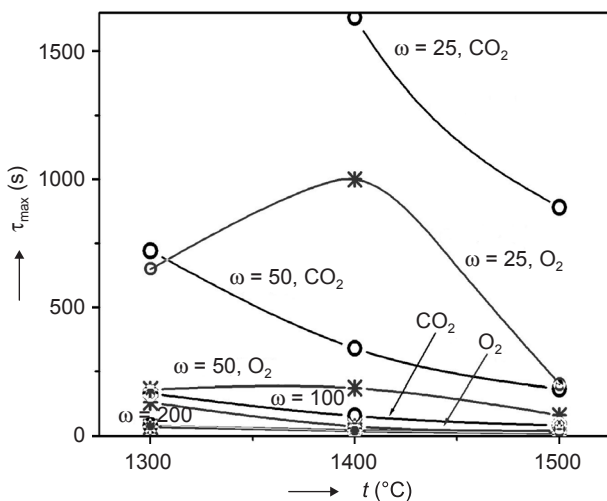


Figure 8. The dependence between the bubble removal time (regardless of the initial bubble radius) and temperature. Oxygen and  $\text{CO}_2$  bubbles,  $V/V_0 = 0.5$ ,  $R_0 = 0.25$  m,  $r_0 = 0.25$  m. The dissolution times are denoted by asterisks, the separation times by circles.

Temperature always plays an important role in bubble behavior, particularly under conditions of chemical solubility of gas in glass melt. The maximum bubble removal times were obtained from calculations of the bubble behavior at different temperatures and the results for the case of standard cylinder ( $R_0 = 0.25$  m) and for initial bubble positions at the cylinder periphery are plotted for both gases in figure 8. The bubble removal times of  $\text{CO}_2$  always decrease with temperature increasing due to decreasing glass viscosity. The removal times of oxygen, however, show maxima or minima at  $1400^\circ\text{C}$  and at lower rotation velocities. The maximum removal times were obtained for bubbles exhibiting the combined removal mechanism: the bubble of the medi-

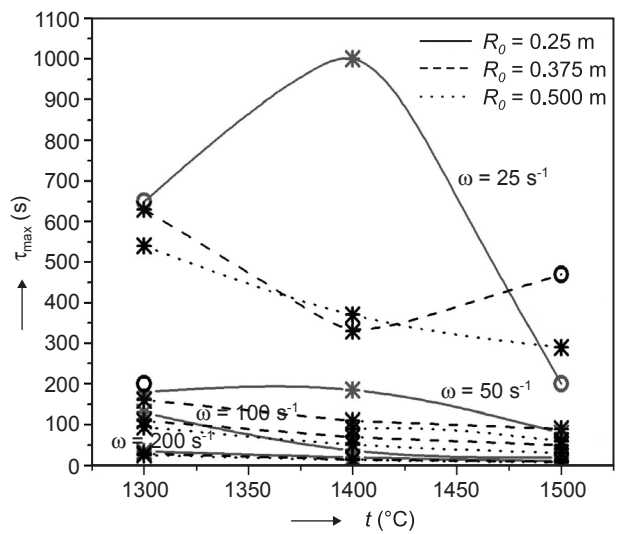


Figure 9. The dependence between the bubble removal time (regardless of the initial bubble radius) and temperature for different radii of the cylinder. Oxygen bubbles,  $V/V_0 = 0.5$ ,  $r_0 = 0.25$  m.

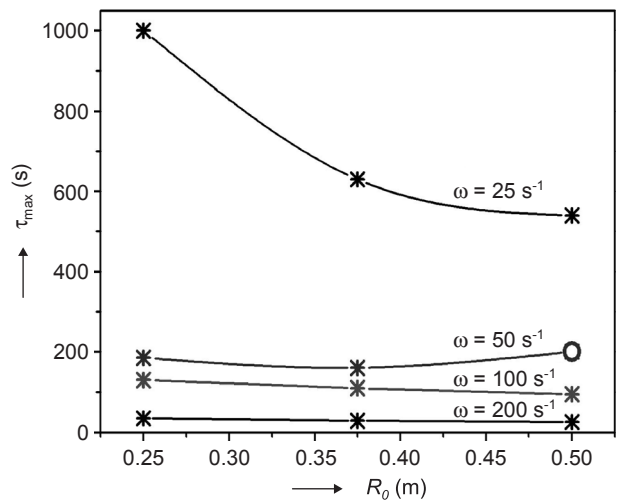


Figure 10. The dependence between the maximum bubble removal time (regardless of temperature and the initial bubble radius) and radius of the cylinder. Oxygen bubbles,  $V/V_0 = 0.5$ .

um radius progressed fairly to the cylinder centre during earlier stages and consequently only slowly dissolved in the melt, the dissolution being the removal mechanism. If, on the contrary, the separation mechanism dominated and bubble partially dissolved during earlier stages, the subsequent separation mechanism is slow and the separation time is high as is demonstrated by the curve for  $\omega = 25 \text{ s}^{-1}$  and  $R_0 = 0.25 \text{ m}$  in figures 8 and 9. Figure 9 summarizes the temperature impact on  $\tau_{max}$  for cylinders having  $R_0 = 0.25, 0.375$  and  $0.5 \text{ m}$ . Both figures 8 and 9 also show that temperature almost stops to be an important factor at higher rotation velocities, characterized by low values of bubble removal times.

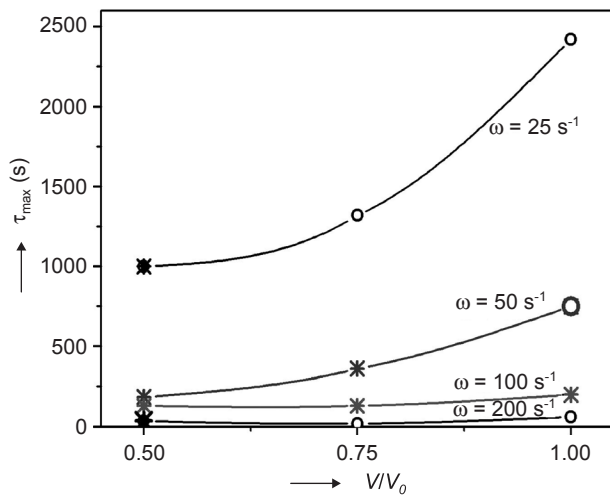


Figure 11. The dependence between the maximum bubble removal time (regardless of temperature and the initial bubble radius) and the degree of cylinder filling by melt. Oxygen bubbles,  $R_0 = 0.25 \text{ m}$ ,  $r_0 = 0.25 \text{ m}$ .

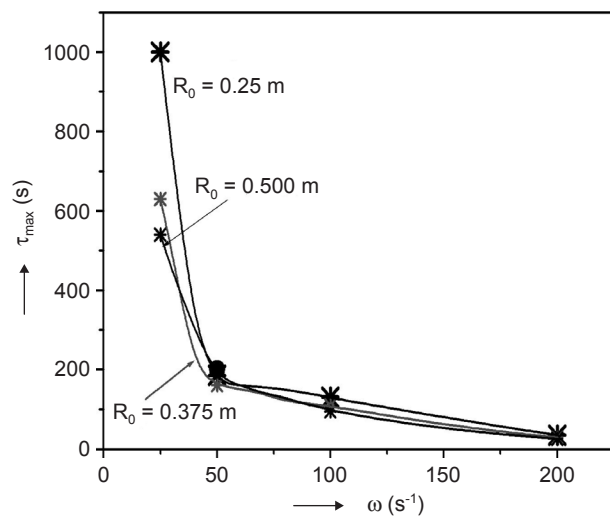


Figure 12. The dependence between the maximum bubble removal time (regardless of temperature and initial bubble radius) and the cylinder rotation velocity. Oxygen bubbles,  $V/V_0 = 0.5$ .

Figure 9 also demonstrates the expected beneficial influence of a greater cylinder radius on the rate of the bubble removal by both mechanisms. The dependence of  $\tau_{max}$  on the cylinder radius at all temperatures and initial bubble radii, and at given value of  $\omega$ , is given by figure 10. The figure reveals that a greater cylinder radius is beneficial at lower rotation velocities, but the tendency is flat for rapid rotations. The impact of the degree of the cylinder filling by melt is obvious from figure 11. The lower filling sets up a thinner glass layer on the cylinder mantle and decreases the bubble separation times.

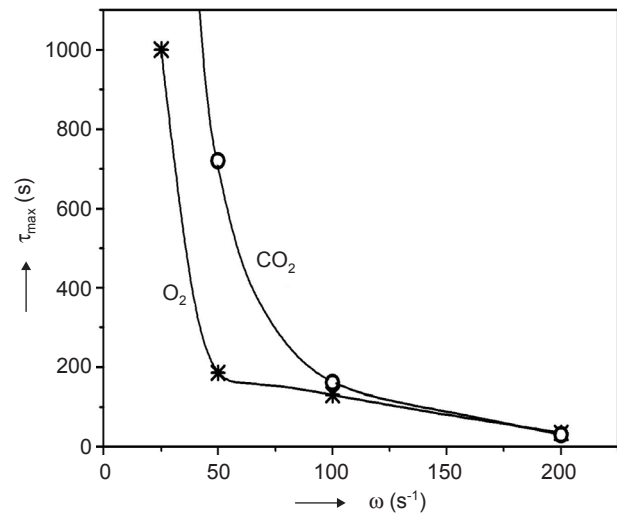


Figure 13. The dependence between the maximum bubble removal time (regardless of temperature and initial bubble radius) and the cylinder rotation velocity. Oxygen and  $\text{CO}_2$  bubbles,  $V/V_0 = 0.5$ ,  $R_0 = 0.25 \text{ m}$ ,  $r_0 = 0.25 \text{ m}$ .

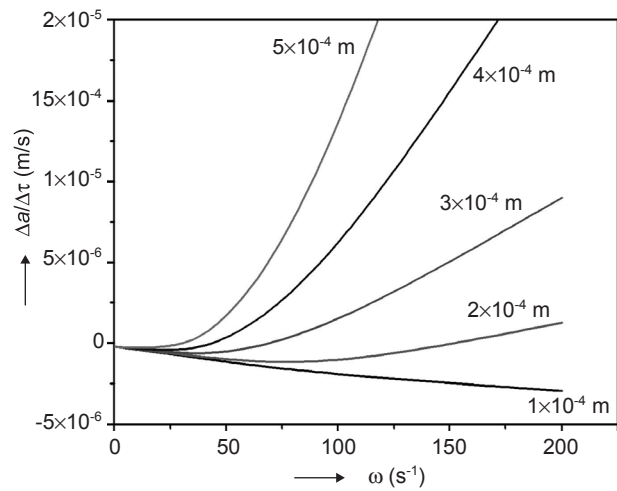


Figure 14. The dissolution and growth rates of oxygen bubbles in the rotating cylinder with glass melt as a function of the cylinder rotation velocity. Temperature  $1300^\circ\text{C}$ ,  $V/V_0 = 0.5$ ,  $R_0 = 0.25 \text{ m}$ ,  $r_0 = 0.25 \text{ m}$ .



The most significant factor of the process appeared to be the cylinder rotation velocity affecting both important phenomena during the bubble removal: the rate of bubble dissolving or growth and bubble movement. Figure 12 demonstrates this fact for oxygen bubbles and for three cylinder radii. The dissolution mechanism of smaller bubbles appeared to be the critical one in most cases. The increase of the rotation velocity from  $\omega = 25 \text{ s}^{-1}$  to  $\omega = 50 \text{ s}^{-1}$  was generally decisive for a substantial decrease of maximum bubble removal times. The different preference of the removal mechanism for oxygen and  $\text{CO}_2$  gas in the standard cylinder  $R_0 = 0.25 \text{ m}$  is obvious from figure 13. The only feasible mechanism for bubbles containing  $\text{CO}_2$  was the separation to the

glass level, this mechanism being slow at lower rotation velocities. That is why only the rotation velocity  $\omega = 100 \text{ s}^{-1}$  decreased the maximum bubble separation times of  $\text{CO}_2$  bubbles to the value standard for oxygen bubbles.

### DISCUSSION

The primitive mechanism of the particle separation from a liquid in rotating cylinders is their wandering to the periphery or the centre of the cylinder due to density differences between particles and liquid, bubbles swimming to the cylinder centre. In addition, the gaseous particles may increase their sizes due to the pressure drop from the cylinder periphery to its centre, and they may dissolve or grow if the gas inside a bubble has a remarkable solubility in the melt, e.g. due to a chemical reaction. The bubbles in glass melt exhibit all the mentioned effects according to bubble and glass properties, and with respect to the parameters of centrifuging. As a result of that, bubbles may disappear from the melt either by the complete dissolution or by the separation to the curved glass level in the cylinder.

The dissolution mechanism is obviously significant for small bubbles under otherwise equal conditions (see figure 3). The wandering of small bubbles in the radial direction is slow (figure 4), the pressure inside a bubble supporting bubble dissolution is therefore high for a long time. As oxygen chemical solubility increases with decreasing temperature and the diffusion coefficient grows, the temperature dependence of bubble dissolution time is less significant. The average dissolution and growth rates of oxygen bubbles at  $1300^\circ\text{C}$  and  $1500^\circ\text{C}$  are presented in figures 14 and 15 as a function of the cylinder rotation velocity. Small bubbles ( $a_0 = 1 \times 10^{-4} \text{ m}$ ) exhibit a slight increase of their absolute values with growing  $\omega$ . The dissolution is partly characteristic also for bubbles with  $a_0 = 2 \times 10^{-4} \text{ m}$  at lower temperatures.

The bubbles of greater sizes grow under identical conditions, even if the gas diffused out of bubbles. The rapid initial radial bubble wandering, results in a pressure drop inside bubbles, which is responsible for a considerable bubble growth. This fact is clear as well from figures 14 and 15 for bubble sizes greater than about  $2 \times 10^{-4} \text{ m}$ . The pressure drop in bubbles, compensated by the growth of bubble size, significantly increases the bubble radial velocity and the bubble quickly reaches the curved glass boundary. The pressure drop decreases towards the cylinder centre and the effect of the centrifugal force is therefore more significant for cylinders having a low filling by glass. The problem occurs with medium bubble sizes, here about  $a_0 = 2 \times 10^{-4} \text{ m}$ , exhibiting both mechanisms in a comparable intensity. The dissolution mechanism is considerably slowed down if a bubble wandered to the glass boundary before (the

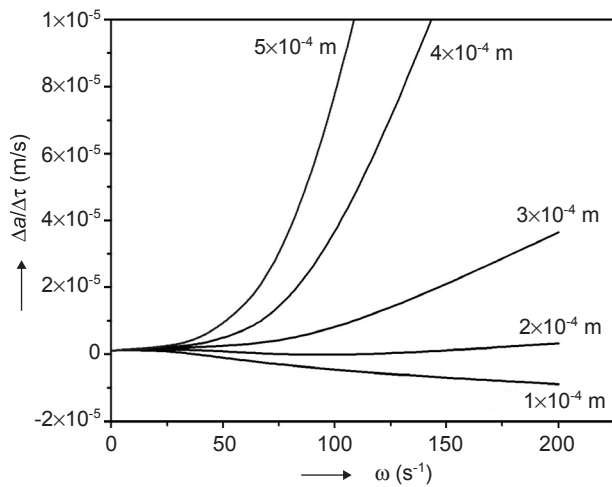


Figure 15. The dissolution and growth rates of oxygen bubbles in the rotating cylinder with glass melt as a function of the cylinder rotation velocity. Temperature  $1500^\circ\text{C}$ ,  $V/V_0 = 0.5$ ,  $R_0 = 0.25 \text{ m}$ ,  $r_0 = 0.25 \text{ m}$ .

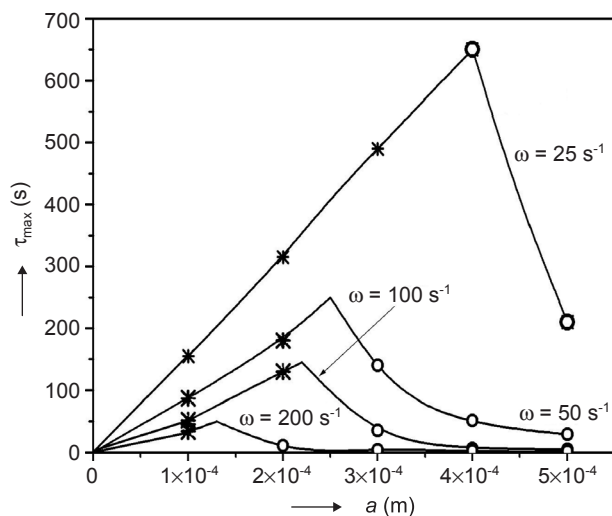


Figure 16. The dependence between the maximum bubble removal time and the initial bubble radius. Oxygen bubble, temperature  $1300^\circ\text{C}$ ,  $V/V_0 = 0.5$ ,  $R_0 = 0.25 \text{ m}$ ,  $r_0 = 0.25 \text{ m}$ .

case of bubble  $a_0 = 2 \times 10^{-4}$  m,  $\omega = 25$  s $^{-1}$  at 1300°C). The separation mechanism is slowed down by bubble's previous partial dissolving in the melt. In order to find the most disadvantageous conditions for the bubble removal, the values of bubble removal times were plotted as a function of the initial bubble radius. The example is provided by figure 16 for the case of  $R_0 = r_0 = 0.25$  m,  $V/V_0 = 0.5$  and temperature 1300°C. The bubble dissolution times (asterisks) in this figure grow linearly with the initial bubble radius whereas the bubble separation times (circles) progressively increase with decreasing initial bubble radius. If both dependences are extrapo-

lated to their intersection, the maximum bubble removal time is found, corresponding to the case when both mechanisms are of equal value. As it is apparent from figure 16, the value of the bubble radius, corresponding to the maximal bubble removal time,  $a_{0max}$ , decreases with growing cylinder rotation velocity, which was also obvious fact at higher temperatures. The dependences between values of  $a_{0max}$  and the cylinder rotational velocity are presented by figure 17 showing that the value of  $a_{0max}$  at high rotation velocities is almost independent of temperature. Notice that the value of  $\tau_{max}$  at 1500°C and  $\omega = 25$  s $^{-1}$  is absent in figure 17 as only the mechanism of the bubble separation is present under these conditions. Despite the fact that two equally realized mechanisms lead to maximal bubble removal times, the bubble removal times are always definite and the acceptable bubble removal conditions for bubbles containing soluble gas may always be found.

The bubble containing gas almost insoluble in the melt exhibits only the separation mechanism. The mechanism is fast, only slightly dependent on temperature, and it is significantly accelerated by the increasing cylinder rotation velocity. However, the problem of the separation of very small bubbles arises as the bubble separation time tends to infinity for the zero bubble size. The dependence between the separation time of the CO<sub>2</sub> bubble and its initial size plotted in a logarithmical form in figure 18 indicates that the problem of the bubble separation may occur for bubbles having the size less than about 0.1 mm.

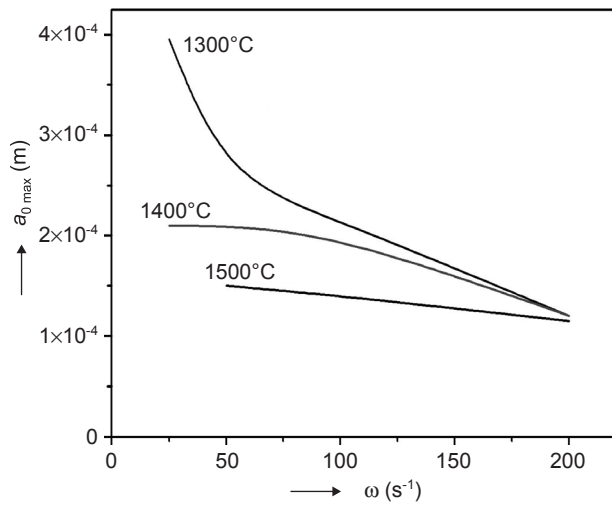


Figure 17. The initial radius of the bubble, characterized by the maximum removal time, as a function of the cylinder rotation velocity. Oxygen bubble,  $V/V_0 = 0.5$ ,  $R_0 = 0.25$  m,  $r_0 = 0.25$  m.

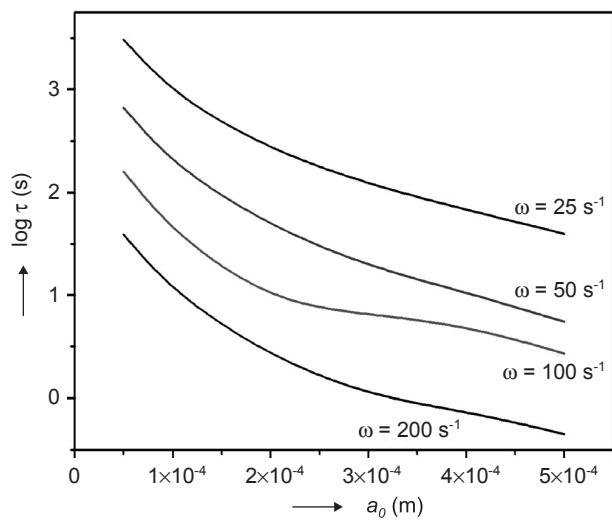


Figure 18. The dependence between the maximum bubble separation time (regardless of temperature) and the initial bubble radius. CO<sub>2</sub> bubbles, temperature 1500°C,  $V/V_0 = 0.5$ ,  $R_0 = 0.25$  m,  $r_0 = 0.25$  m.

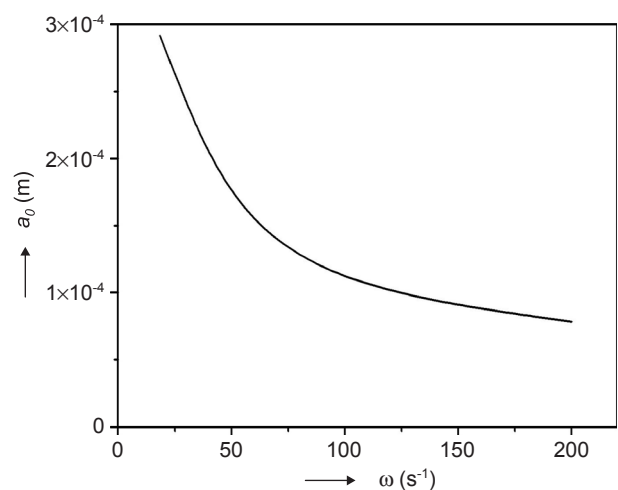


Figure 19. The original bubble radius (at pressure 1 bar) as a function of the cylinder rotation velocity, corresponding to the value of the maximum bubble separation time 1000 s (regardless of temperature), CO<sub>2</sub> bubbles,  $V/V_0 = 0.5$ ,  $R_0 = 0.25$  m,  $r_0 = 0.25$  m.



## CONCLUSION

The main physico-chemical problem bound with the application of the centrifugal force for the bubble removal is the separation of very small bubbles containing slowly diffusing and in melt slightly soluble gas. Only the mechanism of the bubble separation to the cylinder centre is relevant because the bubble dissolution is a too slow process here. The problem with very small bubbles is given by the fact that,  $\tau_{max} \rightarrow \infty$  for  $a_0 \rightarrow 0$  for a totally insoluble gas. This fact should be taken into account as well the fact that the original bubble size decreased due to a pressure increase just after the bubble entered the rotating cylinder. Figure 19 shows the dependence between the original bubble size (at pressure 1 bar) and the cylinder rotation velocity for the bubble removal time  $\tau_{max} = 1000$  s and CO<sub>2</sub> bubbles. The bubbles with the original size smaller than about 0.15 mm already have relatively high separation times even at the rotation velocity of 200 s<sup>-1</sup>. Bubbles in the real melting process always contain a mixture of gases both soluble and almost insoluble in the melt. The problem of a proper initial bubble composition then becomes significant and its solution calls for an examination of the behavior of multi component bubbles in the centrifugal field.

## Acknowledgement

*This work was supported by the research program MSM 6046137302, Preparation and research of functional materials and material technologies using micro- and nanoscopic methods.*

## References

1. Němec L., Tonarová V.: *Ceramics-Silikáty* 49, 162 (2005).
2. Beerkens R.: Proc. 7<sup>th</sup> International Conference on Advances in Vision and Processing of Glass III, Orchester NY, July 27-31, 2003.
3. Ross C.P.: *Am.Ceram.Soc.Bull.* 83, 18 (2004).
4. Kunkle G. E., Welton W. M., Schweninger R. L.: US Pat. 4,738,938 (1988).
5. Kloužek J., Němec L., Ullrich J.: *Glastechn. Ber. Glass Sci. Technol.* 73, 329 (2000).
6. US Pat. 4,316,734.
7. Clift R., Grace J. R., Weber M. E.: *Bubbles, drops and particles*, Academic Press, New York, London 1978.

## ODSTRAŇOVÁNÍ JEDNOSLOŽKOVÝCH BUBLIN ZE SKELNÉ TAVENINY V ROTUJÍCÍM VÁLCI

LUBOMÍR NĚMEC, VLADISLAVA TONAROVÁ

*Laboratoř anorganických materiálů, společné pracoviště  
Vysoké školy chemicko-technologické v Praze  
a Ústavu anorganické chemie AVČR  
Technická 5, 166 28 Praha*

V této práci jsme zkoumali chování bublin obsahujících čistý kyslík nebo oxid uhličitý nacházejících se v rotujícím válci se skelnou taveninou. Pro výpočty chování byla použita rovnice popisující chování bubliny za podmínek ustáleného koncentračního gradientu plynu na povrchu bubliny a za působení odstředivé síly. Vyšetřovali jsme vliv úhlové rychlosti rotace, stupně naplnění válce taveninou, poloměru válce, teploty, počáteční velikosti bublin a jejich počáteční polohy ve válci na dobu potřebou k odstranění bubliny z taveniny s cílem nalézt optimální podmínky pro tento proces. Při odstraňování se uplatnil jak mechanismus úplného rozpuštění některých bublin, tak mechanismus jejich odstředění ke středu válce. Působící mechanismus byl závislý především na počátečním složení bublin. Rozpouštěcí mechanismus byl vedle mechanismu odstředění významný pro bubliny obsahující ve skelné tavenině dobře rozpustný plyn, kterým byl kyslík, zatímco málo rozpustný oxid uhličitý byl odstraňován pouze odstředěním. Oba mechanismy urychlovala zvyšující se rychlost rotace. Aplikace odstředivé síly při výrobě skla vyžaduje zkoumat rovněž chování vícesložkových bublin, jejichž složení odpovídá reálným podmínkám.